EVALUATION OF THERMAL RESISTANCE IN COMMERCIAL HEAT SINKS

Humberto Araujo Machado, humbertoham@iae.cta.br
Instituto de Aeronáutica e Espaço - IAE
Comando-Geral de Tecnologia Aeroespacial – CTA
Pç. Mal. Eduardo Gomes, 50, Vila das Acácias
12.228-904
São José dos Campos, SP

Miguel Hiroo Hirata, hirata@superonda.com.br
Newton G. C. Leite, nleite@uerj.br
Izabel Cristina Loth de Oliveira, Izabel.Oliveira@volkswagen.com.br
Centro de Fontes Renováveis de Energia - CFRE
Departamento de Mecânica e Energia – DME
Faculdade de Tecnologia – FAT
Universidade do Estado do Rio de Janeiro – UERJ
Rodovia Presidente Dutra, km 298, Pólo Industrial
27.537-000
Resende, RJ

Abstract. In this work the behavior of the thermal resistance of commercial heat sinks is studied, concerned to the Reynolds number, fin height and thickness. Theoretical and experimental values of the Nusselt number are compared, after measurements in a low speed wind tunnel, specially constructed and equipped for this experiment. Experimental results show strong fin efficiency dependence to the Reynolds number and some geometric parameters. An uncertainty analysis for the thermal resistance estimative indicates that some adjustments are necessary in the temperature measurements in the heating basement. Although the experimental estimative for Nusselt number presented dispersion when compared to the theoretical ones extracted from a correlation, the results were considered coherent with the literature.

Keywords: thermal resistance, heat sink, cross flow

1. INTRODUCTION

Electronic equipment need some kind of cooling, commonly air flowing through the fins of a heat sink, in order to keep the temperature below the limit of operation. When this limit is surpassed, diverse problems can occur, including the reduction of the component life, working interruption, malfunctioning and even permanent damage. The higher the environment temperature, higher is the temperature reached by the component. Normally, the external temperature is controlled through air conditioning. The internal heating is the result of the summation of all the heat sources assembled: the CPU, Hard disk, CD-Rom, and video boards. Depending on the ventilation, temperature difference can reach 10° C above the environment temperature.

The cooler efficiency can be improved raising its size or reducing the thermal resistance between the cooler and the heat sources. Another way to increase the cooling capacity is improving the performance of the heat sink (Aung, 1991, Steinberg, 1980). Although many studies that includes experimental results are found in literature, the diversity of geometries, arranges and sizes of the commercial heat sinks indicates that the best way to evaluate their performance is to test in real conditions of operation.

In this work, six different types of commercial heat sinks are tested, in order to understand the thermal resistance behavior in different conditions of operation. A low velocity wind tunnel was constructed and equipped for this specific application. The resulting Nusselt numbers are compared with the theoretical forecasts, in order to evaluate the accuracy of the experimental procedure and measurements.

2. EXPERIMENTAL APPARATUS

The test of heat sinks needs equipment that allows simulating a fluid flow in specific conditions. A simple fan would not be appropriate, since it would generate an open air flow, and heat sinks are normally attached in internal spaces, like a computer assemble. Indeed, a specific testing facility should be available for this situation. The small wind tunnel showed in Fig.1 was based in the works of Li and Chao (2009), Li and Chen (2007), Elshafei (2007) and Mohamed (2006). According to the schematics, the air flow is parallel to the fins of the heat sink, although in some cases a impinging jet is observed.

(a)   Lateral view   *(b)   Frontal view*
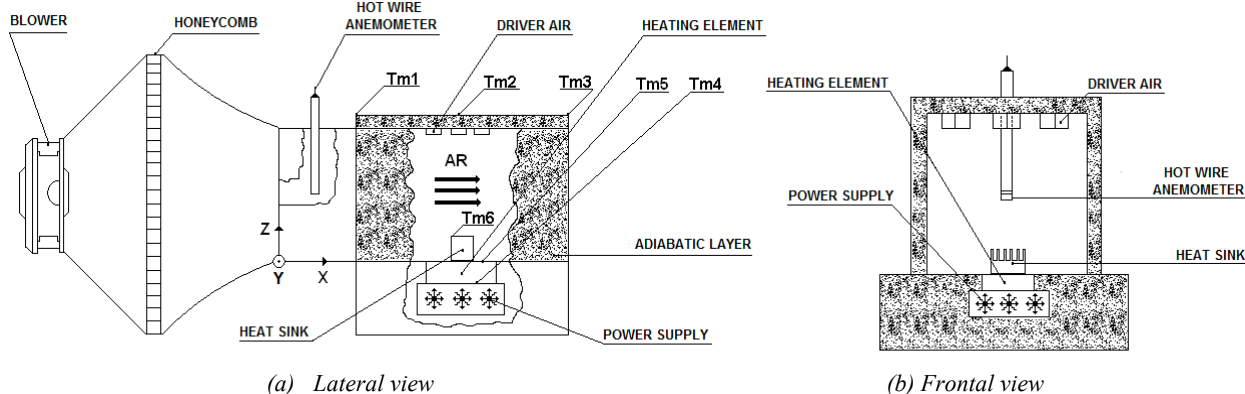
Figure 1. Wind tunnel.

The wild tunnel consists in a flow chamber coupled to duct with a square section. The flow chamber comprehends a axial fan of the *Tarzan AC* family, model TN3A2, a divergent nozzle, a *honeycomb* to keep the flow uniformity and a convergent nozzle. To satisfy specific needs of the project the square section duct coupled to the flow chamber had its inferior wall connected to a heating box, Figs. 1.a,b. This heating box emulates a CPU, releasing heat to the heat sink. It consists in a heat source with adjustable nominal power and the heating basement. The heating basement is a copper block with lateral channels to yield the air flow stagnation, in order to assure the heat flux in the block is one-dimensional in the *z* direction. The heat sink is placed right above the heat basement and is completely exposed to the air flow coming from the flow chamber. As already mentioned, the fins are placed parallel to the air flow.

In the upper wall of the square duct, some flow guides were placed to modify the flow characteristics. However, these guides were not used in this study. Finally, the walls of the square duct were thermally insulated with *isopor* plates.

2.1. Instrumentation and control

Two probes are placed inside the tunnel to follow the flow conditions. The first one was a hotwire anemometer (that was previously calibrated), upward the heat sink in order to measure the velocity and temperature (T_{m1}) at one point within the flow. The anemometer is connected to a multifunctional device model AMI300 by KIMO INSTRUMENTS, employed to convert the signal into velocity and temperature values. A preliminary test demonstrated that the velocity was approximately uniform in the duct section. Indeed, the value measured by the anemometer in the duct centerline was adopted as the average velocity.

The second probe used is a set of thermocouples. These thermocouples were built using naked wires, type J, which were also previously calibrated. Four reference temperatures were used for the calibration: fusion of ice, environment temperature, boiling point of water and the peak temperature reached by the heater. The environment and heater temperatures were measured with a probe model 90013 connected to a Thermo-Collector (TM10) device by Yokogawa M&C Corporation, with excellent accuracy (uncertainty bellow 1° C). Therefore, the thermocouples locally built could have their measurements adjusted from the previous knowledge of the difference between the reference temperatures (extracted from calibrated devices) and their measured values.

A thermocouple named T_{m2} was placed on the duct centerline, right above the heat sink. Another one, T_{m3}, was placed at the end of the duct, in front to the airstream crossing the heat sink. T_{m4} was the average of measurements of four thermocouples placed at every side of the heat basement, at the interface with the heat source. T_{m5} was obtained by a similar way, but the thermocouples were placed at the interface between the heat basement and the heat sink. T_{m6} was the measurement of a thermocouple attached to top of the heat sink fins. The signals collected from the thermocouples were processed by an acquisition system ADS2000 IP along with the programs AqDados 7 abd AqDAnalysis by Lynx Tecnologia Eletrônica Ltda.

The air flow rate in the wind tunnel was controlled through a *dimmer* connected to the fan circuit. This device cuts off the sinusoidal wave, turning off the fan automatically every time the electrical current changes direction, i.e., every time the voltage reaches zero. This happens twice a cycle, turning on the circuit when the voltage reaches a selected level adjusted by the operator through the *dimmer*.

3. HEAT SINKS

Heat sinks to be tested were selected according to the types available in the market. After a previous selection among diverse models, few types were chosen due the geometric and size similarities. Fig. 2 shows one of the selected models.
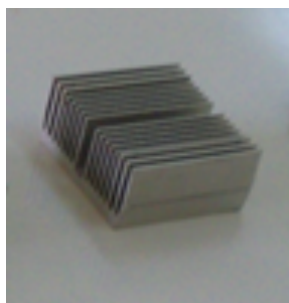
Figure 2. HEAT SINK 1.

The final selection accounted the material, dimensions and channel shape. Six models made with aluminium were selected. Their characteristics are shown in Tab. 1.

Tab 1. Characteristics of selected heat sinks.

HEAT SINK	$L_x 10^2$ [m]	$L_y 10^2$ [m]	$L_z 10^2$ [m]	$E_a 10^3$ [m]	$E_b 10^3$ [m]	N
1	5.0	5.1	2.0	1.3	5.0	16
2	6.8	7.7	3.1	1.0	12.0	29
3	4.75	4.9	2.1	0.11	0.4	20
4	5.9	6.0	2.4	0.1	---	28
5	3.7	3.7	1.2	0.1	0.3	07
6	7.6	4.5	2.1	0.1	---	29

Dimensions L_x, L_y and L_z represent the lengths in the respective directions, where L_z refers only to the fin height (without accounting base thickness). In the case of heat sinks with variable fin height, the value shown in Tab. 1 refers to the average between the biggest and smallest values found in the heat sink. E_a is the mean thickness of the fins and E_b is the mean thickness of the base. N is the number of fins in the heat sink.

4. METHODOLOGICAL STUDY

The thermal resistance of the heat sink is calculated through the combination of the thermal resistances defined in Fig. 3: R_{base}, representing the conductive resistance of the heat sink base; $R_{effective}$, representing a series of resistance in parallel that include the conducive fin resistances and the convective resistance of the channels between the fins (interstices) and $R_{convective}$ representing the convective resistance between the heat sink and the fluid flowing above.
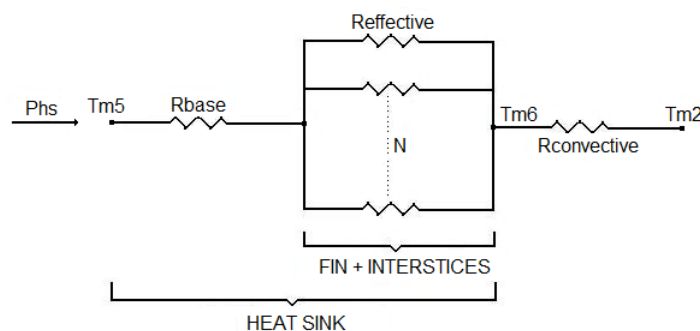
Figure 3. Analogy between thermal resistance and an electrical circuit.

While R_{base} is a constant, $R_{effective}$ and $R_{convective}$ are dependent on the flow in the test section. The value of the heat sink thermal resistance will be the summation of the three serial resistances shown in Fig. 3:

$$R = R_{base} + R_{effective} + R_{convective} = \frac{T_{m5} - T_{m2}}{P_{dis.}}$$ (1)

The total amount of heat transferred by the heat sink (P_{hs}) is indirectly estimated through the Fourier law applied into the heating base:

$$P = -\kappa_{copper} A_{copper} \frac{\partial T}{\partial z} = \kappa_{copper} A_{copper} \frac{(T_{m4} - T_{m5})}{\Delta z} \tag{2}$$

where P is the heating power released by the heating base, κ_{copper} is the copper thermal conductivity, A_{copper} is the area of the surface perpendicular to the heat and Δz is the heating base thickness.

Once P is known, the heat flux can also be determined. Assuming that the heat flux is uniform in the while heating base, P_{hs} can be estimated:

$$P_{hs} = \frac{P}{A_{copper}} A_{hs} \tag{3}$$

where A_{hs} is area of the heat sink that is perpendicular to the heat flux, i.e., the contact area with the heating base.

Theoretical Nusselt number was estimated through its definition:

$$Nu_{teór.} = \frac{h_{teór.} L_x}{\kappa_{ar}} \tag{4}$$

where κ_{air} is the thermal conductivity of the air and $h_{teór.}$ was estimated through a correlation (Subramanyam and Crowe, 2000):

$$h_{theor} = 0{,}664 \frac{k_{air}}{L_x} \mathrm{Re}_{L_x}^{\frac{1}{2}} \mathrm{Pr}^{\frac{1}{3}} \tag{5}$$

The Prandt number (Pr) was extracted from literature, while the Reynolds number (Re_{L_x}) was defined as:

$$\mathrm{Re}_{L_x} = \frac{V_{anem.} L_x}{\nu_{ar}} \tag{6}$$

where $V_{anem.}$ Is the mean air velocity measured with the use of the hot wire anemometer, as mentioned before, and ν_{air} is the kinematic viscosity of the air. For the graphic presentation of the thermal resistance x Reynolds number, in the following sections, Eq.(6) was modified, replacing L_x by the length of the test section sides.

Experimental Nusselt number was calculated as:

$$Nu_{exp.} = \frac{h_{exp.} L_x}{\kappa_{air}} \tag{7}$$

Every thermophysical properties of the air were estimated at the mean average of the environment temperature, defined as:

$$\overline{T}_{air} = \frac{T_{m1} + T_{m2} + T_{m3}}{3} \tag{8}$$

The experimental film coefficient ($h_{exp.}$) was estimated as:

$$h_{exp.} = \frac{P_{hs}}{A_{hs\_total} (T_{m5} - T_{m2})} \tag{9}$$

where A_{hs_total} is the contact area between the fluid and the heat sink (fins + interstices), which has to be calculated. All the experimental measurements were done after steady state was reached.

4.1. Analysis of uncertainty

The error bars of for the experimental values of the thermal resistance were calculates through the following expression:

$$u_R = \pm \left[\left(\frac{T_{m5}}{R} \frac{\partial R}{\partial T_{m5}} u_{Tm5} \right)^2 + \left(\frac{T_{m2}}{R} \frac{\partial R}{\partial T_{m2}} u_{Tm2} \right)^2 + \left(\frac{P_{hs}}{R} \frac{\partial R}{\partial P_{hs}} u_{Phs} \right)^2 \right]^{\frac{1}{2}}$$
(10)

The same estimative was done for the Reynolds number, resulting in a maximum uncertainty of 3.1 %.

5. RESULTS AND DISCUSSION

Figs. 4-6 show the results for experimental thermal resistance as function of Reynolds number, for peers of heat sinks. Considering the fin height L_z and the fin thickness E_a shown in Tab. 1, thermal resistance decreases with the increase of the first and increases with the second one, for the same Reynolds number. The last effect is evident when heat sinks 1 and 6 are compared for a Reynolds number above 50,000. Thermal resistance fall with Reynolds number until reaches an asymptotic value, which implies in limit of improving the heat sink performance through the raising of the flow velocity.

Figs. 7-9 compare the theoretical forecasts with experimental results for Nusselt number. In this study, the results were considered as preliminary results, since the main objective was to test the methodology and the accuracy of the experimental set up. Although the behavior of the experimental points is similar to theoretical forecasts, results were not considered satisfactory.

Heat sink 5 was the only that has presented atypical behavior, i.e., experimental Nusselt number values were found to be higher than theoretical ones. Such a behavior may be a consequence of heat sink geometry, with small height (L_z) and thickness of the fins (E_a), what resulted in a higher performance, and a lower slope for the path formed with the experimental points.

A hypothesis for the distance between experimental and theoretical values for the Nusselt number is that Eq. 5 does not fit well the heat sinks tested. One option to proof such hypothesis is to find more correlations for comparison. The use of the commercial heat sinks, which is supposed to be one of the objectives of this work, also difficult the parameterization and consequently the extraction of the specific results for thermal resistance and Nusselt number.

6. CONCLUSIONS

In this work a low velocity small wind tunnel was used to evaluate the thermal resistance of commercial heat sinks used in electronic equipment. The experimental set up and procedure were described. Results are coherent with the theoretical forecasts, although the values found were not considered satisfactory. The causes of the deviation can be the correlation used to estimate the theoretical Nusselt number and the dimensions employed in the parameterization.

Concerned to the uncertainties of the thermal resistances, it rises greatly when the Reynolds number decreases to low values, and the maximum value reached was 40 %. It was verified that this parameter is sensitive to the temperature difference in the heating base. Future works shall be focused in the reduction of this sensitiveness, in order to improve the accuracy of the results.
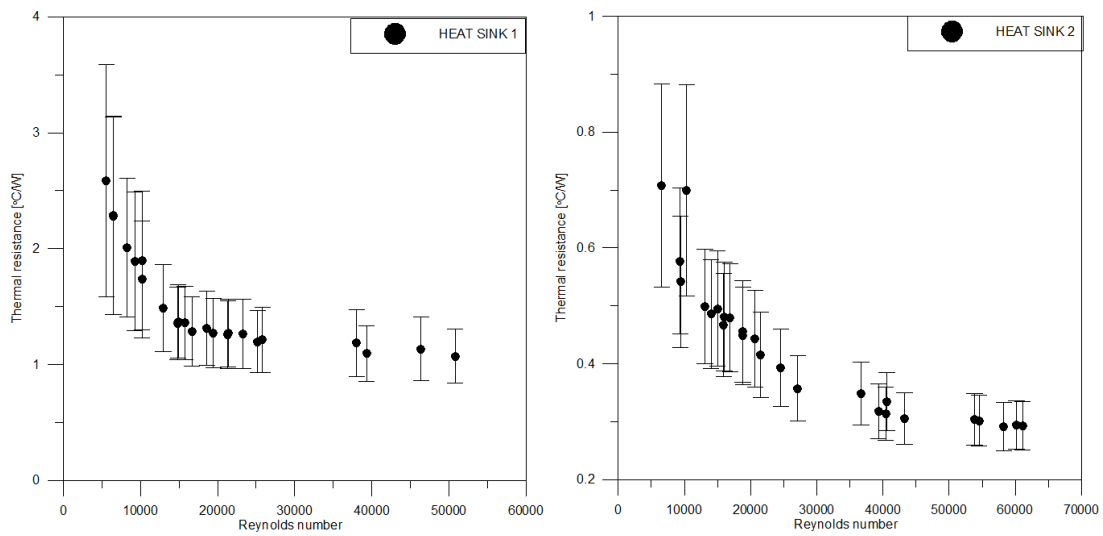
Figure 4. Effect of the Reynolds number variation over the thermal resistance – HEAT SINK 1 e 2.
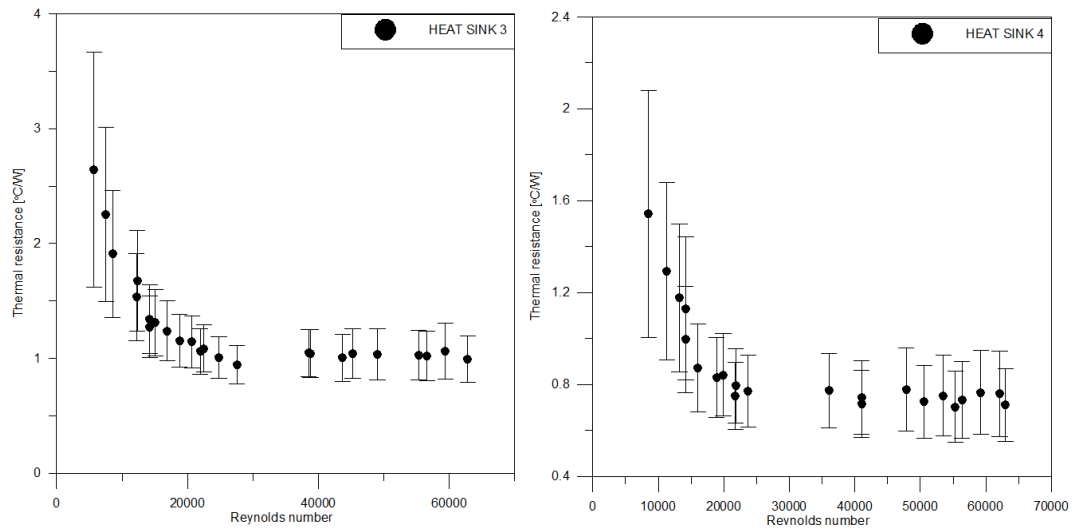
Figure 5. Effect of the Reynolds number variation over the thermal resistance – HEAT SINK 3 e 4.
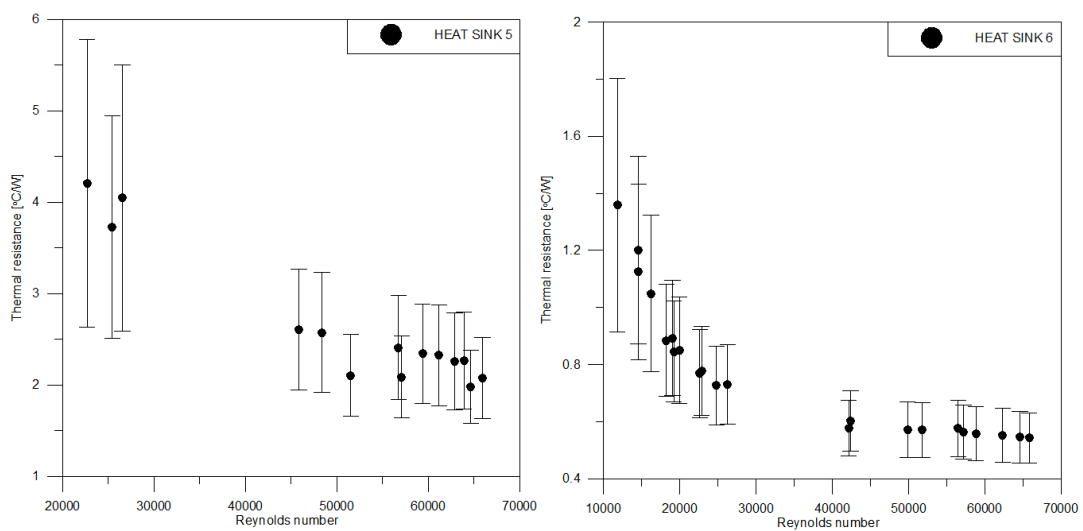
Figure 6. Effect of the Reynolds number variation over the thermal resistance – HEAT SINK 5 e 6.
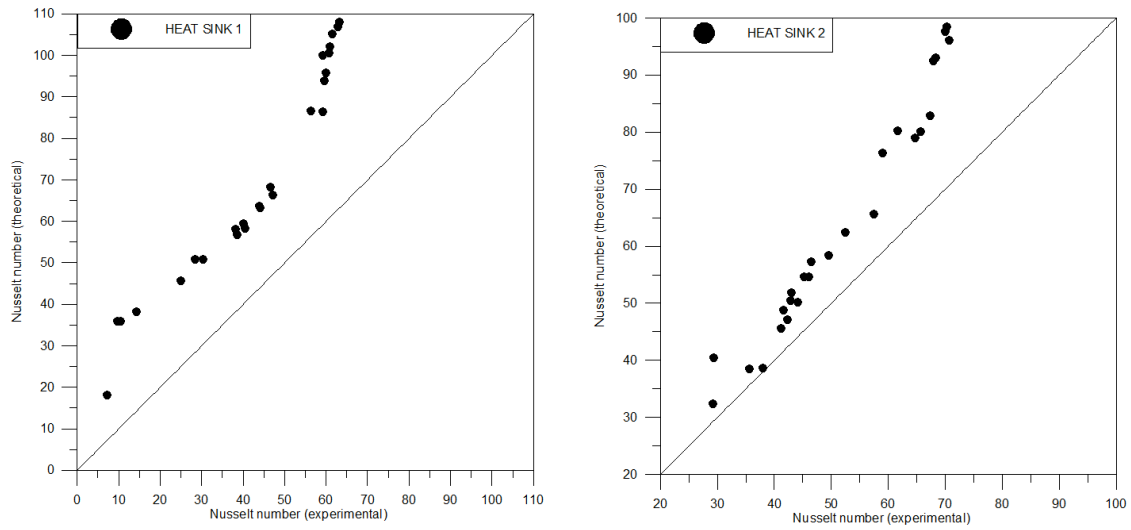
Figure 7. Deviation between experimental and theoretical Nusselt numbers – HEAT SINK 1 e 2.
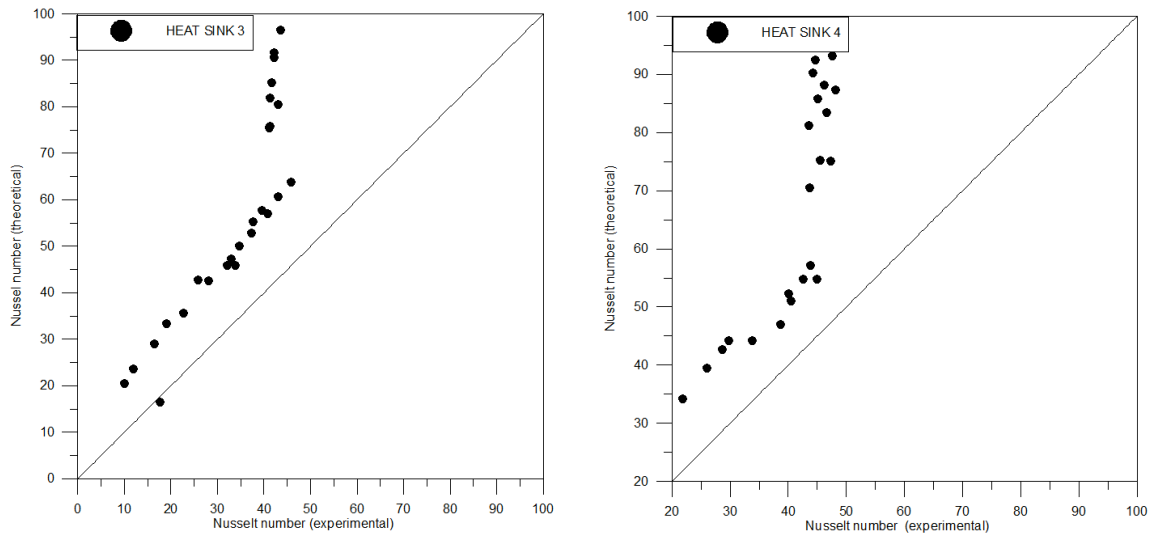
Figure 8. Deviation between experimental and theoretical Nusselt numbers – HEAT SINK 3 e 4.
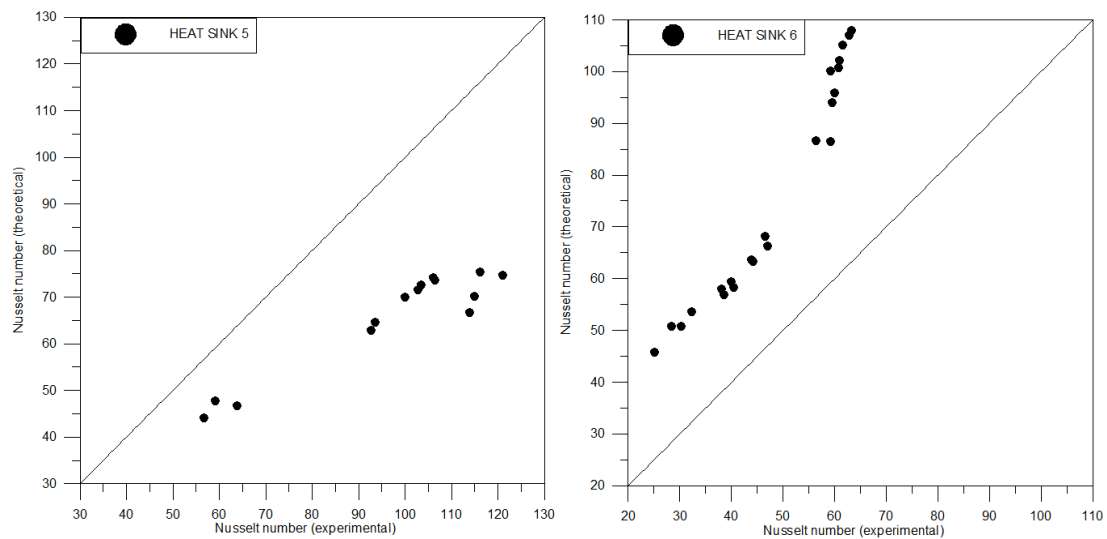
Figure 9. Deviation between experimental and theoretical Nusselt numbers – HEAT SINK 5 e 6.

7. REFERENCES

Aung, W., 1991. Cooling techniques for computers. Hemisphere publishing corporation, New York.

Elshafei, E. A. M., 2007. "Effect of flow bypass on the performance of a shrouded longitudinal fin array". Applied Thermal Engineering, Vol. 27, pp. 2233-2242.

Li, Hung-Yi and Chao, Shung-Ming, 2009. "Measurement of performance of plate-fin heat sinks with cross flow cooling". International Journal of Heat and Mass Transfer, Vol. 52, pp. 2949-2955.

Li, Hung-Yi and Chen, Kuan-Ying, 2007. "Thermal performance of plate-fin heat sinks under confined impinging Jet conditions". International Journal of Heat and Mass Transfer, Vol. 50, pp. 1963-1970.

Mohamed, M. M., 2006. "Air cooling characteristics of a uniform square modules array for electronic device heat sink". Applied Thermal Engineering, Vol. 26, pp. 486-493.

Steinberg, D. S., 1980. Cooling techniques for eletronic equipment. John Wiley & Sons, New York.

Subramanyan, S. and Crowe K. E., 2000. "Rapid design of heat sinks for electronic cooling using computational and experimental ". Sixteenth IEEE SEMI-THERM^{TM} Symposium, pp. 243-251.

8. RESPONSIBILITY NOTICE

The authors are the only responsible for the printed material included in this paper.